Paleozoic tectonic evolution of the northern Xinjiang, China: Geochemical and geochronological constraints from the ophiolites

Zhihong Wang, Shu Sun, Jiliang Li, Quanlin Hou, Kezhang Qin, Wenjiao Xiao, and Jie Hao

Laboratory of Lithosphere Tectonic Evolution, Institute of Geology and Geophysics, Chinese Academy of Sciences, Beijing, People's Republic of China.

Received 9 April 2002; revised 9 December 2002; accepted 5 March 2003; published 22 April 2003.

[1] The northern Xinjiang of China is a composite orogenic belt in the south central part of the Altaids formed by subduction-accretion mainly during the Paleozoic. Geochronologic and geochemical data from the Paleozoic ophiolites and associated assemblages are reported here to place constrains on the tectonic evolution of this region and to reconstruct its history, using a model of subduction-accretion plus large-scale map-view strike-slip faulting. Geologic and geochronologic review indicates that the Paleozoic ophiolites and associated assemblages of the western and eastern Junggar regions are tectonically related, occurring as a pattern with the early Paleozoic Tangbale-Mayile-Hongguleleng-Aermantai complexes in the center, the late Paleozoic Darbut-Karamaili and the northern Tianshan complexes in the south, and the late Paleozoic Kekesentao-Qiaoxiahala-Kuerti complexes in the north. Available geochemical data suggest that the Paleozoic ophiolites of the northern Xinjiang are mainly oceanic fragments of these three types: mid-ocean ridge basalt, oceanic island basalts, and island arc basalts. The Paleozoic subduction-accretion complexes grew mainly along different segments of the Kipchak arc, and in associated with migration of magmatic arc. The Paleozoic ophiolite-associated sedimentary sequences and subduction-related volcanic rocks exhibit an evolution history from intraoceanic (early Paleozoic) to marginal settings (late Paleozoic), implying coeval strike-slip stacking with subduction-accretion processes, and by which to transport the respective complexes together and further to amalgamate with neighboring units of the Altaids. Subduction-accretion processes terminated in the mid-Carboniferous in this region. In the late Permian-early Triassic, a counterclockwise rotation of fault blocks in a giant sinistral strike-slip and extension domain between Altay and Tianshan, lastly generated present configuration of the Paleozoic subduction-accretion complexes in the northern Xinjiang. *INDEX TERMS:* 8110 Tectonophysics: Continental tectonics—general (0905); 8120 Tectonophysics: Dynamics of lithosphere and mantle—general; 8102 Tectonophysics: Continental contractional orogenic belts; 1065 Geochemistry: Trace elements (3670); 1035 Geochemistry: Geochronology; *KEYWORDS:* northern Xinjiang, Paleozoic, ophiolite, subduction-accretion, Altaids. **Citation:** Wang, Z., S. Sun, J. Li, Q. Hou, K. Qin, W. Xiao, and J. Hao, Paleozoic tectonic evolution of the northern Xinjiang, China: Geochemical and geochronological constraints from the ophiolites, *Tectonics*, *22*(2), 1014, doi:10.1029/2002TC001396, 2003.

Copyright 2003 by the American Geophysical Union.
0278-7407/03/2002TC001396$12.00

1. Introduction

[2] The northern Xinjiang geographically occupies the northwest extreme edge of China and geologically is located in the south central part of the Altaids (Figure 1). As a key area for unraveling tectonic framework and evolution of the most interior part of the Eurasian continent, it has received extensive attention by international geologists at the end of eighties, especially the western Junggar region [e.g., *Coleman*, 1989; *Feng et al.*, 1989; *Kwon et al.*, 1989]. However, it has been kept out of the geologists' sight of the western world for a long period after that, even in synthesized palinspastic reconstruction models of China [e.g., *Yin and Nie*, 1996; *Li*, 1998], except for in models of Central Asia or the Altaids [e.g., *Allen et al.*, 1995; *Şengör and Natal'in*, 1996a, 1996b] and recent research on Phanerozoic granitoids in the region [e.g., *Jahn et al.*, 2000; *Hu et al.*, 2000; *Chen et al.*, 2000]. On the other hand, the mechanism of continental growth of Central Asia is currently debated between models invoking continuous subduction-accretion [*Şengör et al.*, 1993; *Şengör and Natal'in*, 1996a, 1996b], or punctuated accretion due to closure of multiple ocean basins. The purpose of this paper is to establish the Paleozoic patterns of crustal development and accretion of this area, using available geochemical and geochronological data mainly from the ophiolites, since ophiolites typically represent offscraped fragments in accretionary complexes or collisional sutures.

2. Major Problems and Controversies

[3] Several important problems and controversies are hotly debated in dealing with the tectonic evolution of the northern Xinjiang:

[4] 1. The original configurations of the ophiolite belts with different ages: Previous tectonic reconstructions have mostly assumed that the present geometry of the ophiolite

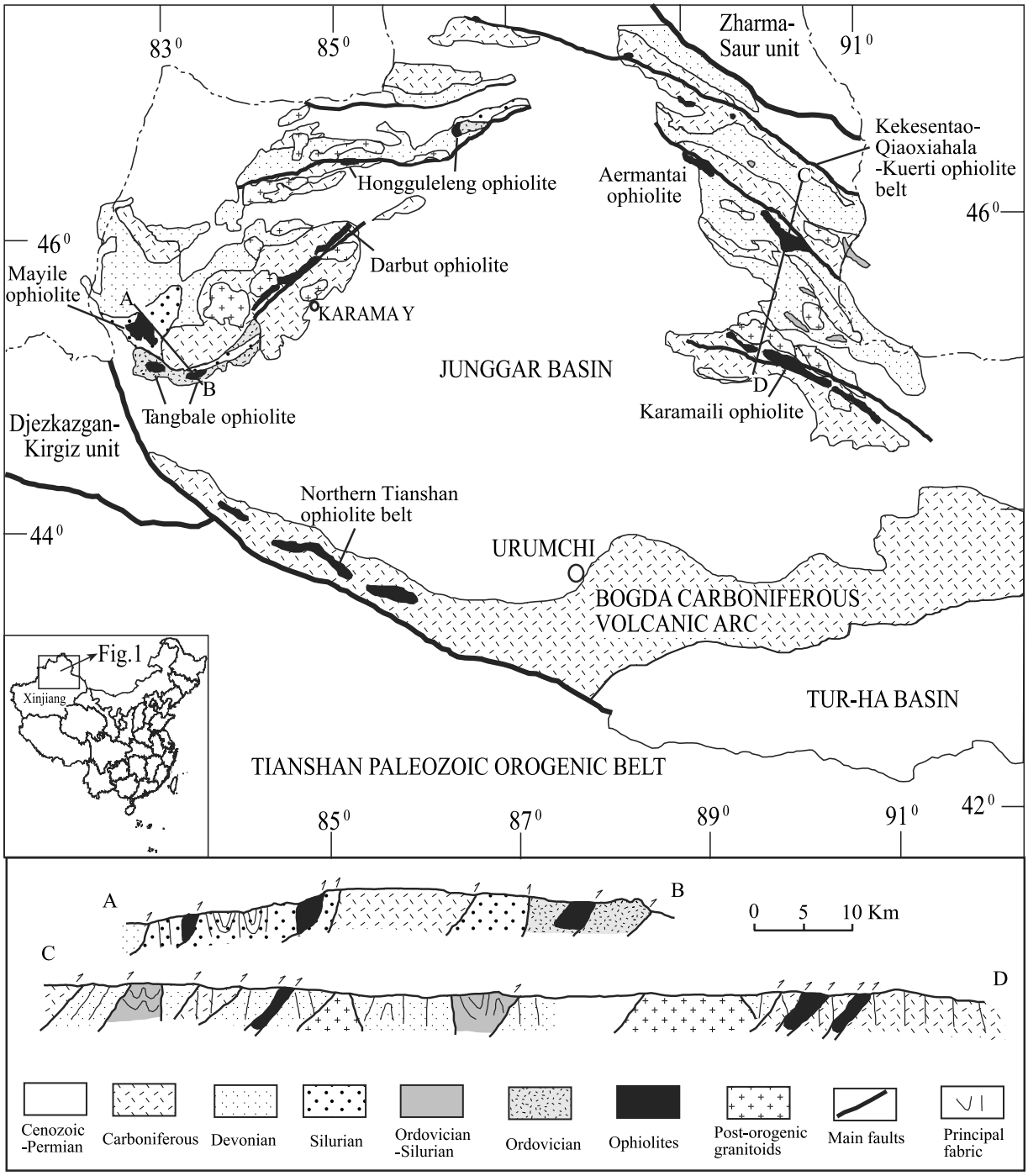


Figure 1. Geological and tectonic map of the northern Xinjiang, China (modified after *Wang et al.* [1995]). The two cross sections are mainly modified after *Li et al.* [1987], *Feng et al.* [1989], and *Li et al.* [1990].

belts represents their original configurations at the time of formation [e.g., *Feng et al.*, 1989; *Zhang et al.*, 1995]. It could be suitable for the eastern Junggar ophiolite belts, whereas the original configurations of the ophiolite belts in the western Junggar region possibly had been extensively affected by rotation of fault blocks in late Permian-early Triassic [*Allen et al.*, 1995].

[5] 2. The formation and accretion of the region: Was it formed by multiple collisions of some microcontinental blocks or terranes [e.g., *Zhang et al.*, 1995; *He et al.*, 1994] or by subduction-accretion processes within the framework of the Altaids [e.g., *Şengör and Natal'in*, 1996a, 1996b], or by collapse of multiple back arc basins.

[6] 3. The nature of the basement of the Junggar basin: Was it a Precambrian metamorphic continental basement [e.g., *Zhang et al.*, 1995] or accreted oceanic crust [e.g., *Coleman*, 1989; *Kwon et al.*, 1989; *Hu et al.*, 2000] or relict and trapped back arc basin [e.g., *Hsu*, 1988; *Feng et al.*, 1989].

[7] 4. The timing of formation and emplacement of the ophiolites: Were there any Precambrian ophiolites as suggested by *Huang et al.* [1999] for the Hongguleleng ophiolite, or were all the ophiolites Paleozoic as proposed by most researches [e.g., *Coleman*, 1989; *Feng et al.*, 1989; *Zhang et al.*, 1995; *Xiao et al.*, 1991; *He et al.*, 1994]. When did the respective ophiolites got emplaced and was there any ophiolite indicative of final suturing.

[8] 5. The origin and tectonic implication of the ophiolites: Did all the ophiolites form in ''limited ocean basins'' [*Xiao et al.*, 1991; *Li*, 1991] or marginal arc-basin systems [e.g., *Feng et al.*, 1989] similar to the present Western Pacific, or in a big ocean and later they were accreted to be subduction-accretion complexes [*Şengör and Natal'in*, 1996a, 1996b].

[9] 6. The Paleozoic tectonic evolution of the western and eastern Junggar areas: The difference of present geometry of the ophiolite belts between the western (more complicated, obviously accommodated by strike-slip faults related to later tectonic events) and eastern (linear) Junggar areas prompted some researches to put forward different patterns of tectonic evolution, though most of them considered that the Darbut ophiolite was tectonically conjoined with the Karamaili ophiolite in the Devonian [e.g., *Xiao et al.*, 1991].

[10] Presently available data can shed much light on most of the problems, and this paper is an attempt to unravel these controversies.

3. Geological Setting

[11] The geology of the northern Xinjiang is characterized by considerable development of ophiolites and related volcanic and volcanoclastic sequences. The lithotectonic unites of the ophiolites and associated sequences were well summarized in previous studies [e.g., *Feng et al.*, 1989; *Xiao et al.*, 1991; *Li*, 1991; *Zhang et al.*, 1995]. Here, we briefly introduce regional geology associated with the ophiolites. In general, the main lithotectonic units within the studied area are: Ordovician to Cenozoic-Permian rock sequences, ophiolites ranging from early to late Paleozoic in age, and late Carboniferous-Permian post-orogenic granitoids (Figure 1).

[12] Ordovician unit occurs restrictively around the Tangbale and Hongguleng ophiolites, and mainly basaltic to andesitic volcanic rocks, radiolarian cherts, turbidites and limestones. Silurian sequence also occurs around the Tangbale, Hongguleng and Mayile ophiolites but displays different lithology. Silurian rocks are mainly early-Silurian flysch-type deposits with ophiolitic debris unconformably overlaid the Tangbale ophiolite, and mainly mid-Silurian pillow lavas and radiolarian cherts interlaying flysch of early and late Silurian at Mayile, while at Hongguleleng mainly andesitic volcanic and volcanoclastic rocks and limestones. In the eastern Junggar, the undivided Ordovician-Silurian sequences, which distributed along the Aermantai ophiolite belt, are mainly andesitic to felsic volcanic and volcanoclastic rocks, cherts, flysch and limestones.

[13] Devonian unit widely occurs in this region but shows different lithology at different areas. At the Darbut area, early-middle Devonian sequence is composed of pillow lavas, radiolarian cherts and limestones, and covered by late Devonian flysch. Clastic sediments and marine flysch with silicic pyroclastics of mid-Devonian unconformably overlie the Ordovician and Silurian rocks at the Mayile and Tangbale areas. Devonian rocks are mainly flysch, clastic sediments intercalated with limestones and tuffs, and andesitic volcanic rocks at the Hongguleleng area. To the north, mid-Devonian mafic to intermediate lavas and cherts are closely associated with the western segment of the Kekesentao-Qiaoxiahala-Kuerti ophiolite belt. In the eastern Junggar, Devonian rocks display a similar lithological pattern with that of the western Junggar. Devonian ophiolitic turbidites, limestones and intermediate to felsic volcanic and volcanoclastic rocks occurred closely with the Karamaili ophiolite in the south. Clastic sediments, limestones, and intermediate to felsic volcanic and volcaniclastic rocks unconformably overlie the Ordovician-Silurian rocks around the Aermantai ophiolite in the middle. Devonian arc volcanic rocks occurred closely with the eastern segment of the Kekesentao-Qiaoxiahala-Kuerti ophiolite belt in the north.

[14] Carboniferous unit is mainly terrestrial clastic sediments in the Junggar region. In the north of the Tianshan Paleozoic orogenic belt, Carboniferous rocks are mainly volcanic and volcaniclastic rocks and turbidites closely associated with the northern Tianshan ophiolite belt at the western segment, and constitute the Bogda volcanic arc at the eastern segment.

[15] The Permian-Cenozoic unit consists of terrestrial volcanic and volcanoclastic rocks of Permian, and alluvial, fluvial and lacustrine deposits after Permian. The Paleozoic ophiolites and late Carboniferous-Permian post-orogenic granitoids will be discussed later.

4. Formation Ages of the Ophiolites in the Northern Xinjiang

[16] In this section, we will mainly synthesize the time data for the ophiolites, and further to constrain their formation ages.

4.1. Early Paleozoic Ophiolites

[17] The Tangbale ophiolite was regarded as the oldest ophiolite in the northern Xinjiang by most researches [e.g., *Coleman*, 1989; *Feng et al.*, 1989; *Kwon et al.*, 1989; *Xiao et al.*, 1991; *Li*, 1991; *Zhang et al.*, 1995]. The formation age of late Cambrian-Ordovician can be constrained using the following evidence: (1) Pb-Pb dating for plagioclase and sphene from the Tangbale leucogabbro gives its formation age in the range of 523–508 Ma [*Tilton et al.*, 1986; *Kwon et al.*, 1989]. (2) A Sm-Nd mineral–whole-rock inner isochron age for the gabbros and a whole-rock isochron age for the basalts are 489 Ma and 447 Ma, respectively [*Zhang et al.*,

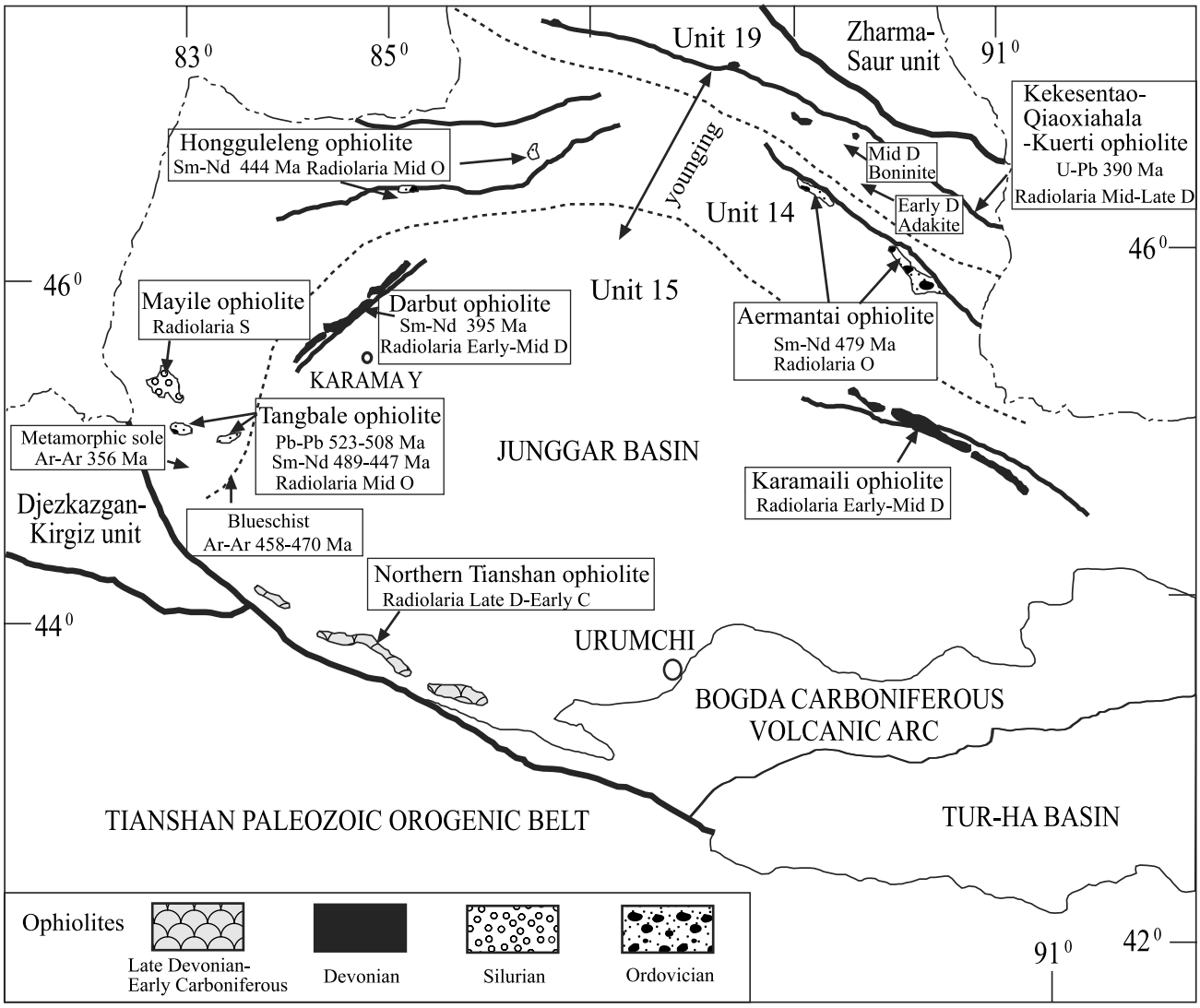


Figure 2. Compiled age data for the ophiolites and related assemblages. Units 14, 15 and 19 are cited from *Şengör and Natal'in* [1996b].

1995]. (3) Ar-Ar dating for sodic amphibole from the blueschists, which occur in the Tangbale ophiolite melange (Figure 2) and possibly resulted from subduction of ocean crust, indicates that this high-pressure metamorphism took place in the range of 458–470 Ma [*Zhang*, 1997]. (4) Radiolaria fossils of middle Ordovician were found in the cherts from the Tangbale ophiolite melange, which stratigraphically intercalate with or overlie the mafic lavas [*Feng et al.*, 1989; *Xiao et al.*, 1991; *Zhang et al.*, 1995].

[18] The formation age of the Hongguleleng ophiolite has not well constrained by geochronologic data. Sm-Nd dating for the cumulate rocks is controversial. An isochron age of 626 ± 25 Ma was given by troctolite, gabbro, plagiogranite and anorthosite [*Huang et al.*, 1999]. However, *Zhang et al.* [1995] reported a Sm-Nd isochron age of 444 ± 27 Ma given by troctolite, gabbro and basalt. Because of lack of detailed geochemical data for these dated rocks, we can not make a concrete choice for these two ages. Middle Ordovician fossils were discovered in the andesitic volcanics [*Bai et al.*, 1986; *Xiao et al.*, 1991], which occur as melange together with the ophiolite (Figure 1), indicating that the ophiolite was possibly formed before the middle Ordovician.

[19] Sm-Nd dating for the harzburgite and dunite in the Aermantai ophiolite presents an isochron age of 479 ± 27 Ma [*Liu and Zhang*, 1993]. Detailed Sm-Nd and Rb-Sr isotopic analyses for the cumulate rocks and mafic lavas were conducted by *Huang et al.* [1997]. A whole-rock isochron age of 561 ± 41 Ma was given by the cumulate gabbro, diabase and andesite porphyrite, and was interpreted as formation age of the ophiolite [*Huang et al.*, 1997]. Rb-Sr dating for the diabase and andesite porphyrite gives a whole-rock isochron age of 392 ± 17 Ma interpreted as the time of later metamorphism [*Huang et al.*, 1997]. The described geochemistry for the dated rocks shows that the cumulate rocks have LREE-depleted or flat REE patterns, whereas the diabases and andesite porphyr-

ites are LREE-enriched [*Huang et al.*, 1997], possibly suggesting that the cumulate rocks and the extrusive rocks are not cogenetic and the whole-rock Sm-Nd isochron for these rocks is probably a false isochron. It is worth to noting that, *Huang et al.* [1997] also calculated a mineral-whole-rock Sm-Nd inner isochron age of 478.9 Ma for the cumulate pyroxene peridotite, concordant with that of the mantle peridotites [*Liu and Zhang*, 1993], though they regarded this age as a metamorphic age. Ordovician radiolaria fossils found in the ophiolite melange [*Li*, 1991], further indicating that the Aermantai ophiolite arguably formed at least in the Ordovician.

[20] Because of lack of any isotopic dating, the time of the Mayile ophiolite is still not well constrained. The discovery of Silurian radiolaria fossils in the cherts from the ophiolite melange indicates that it may form in the Silurian [*Feng et al.*, 1989; *Xiao et al.*, 1991; *He et al.*, 1994; *Zhang et al.*, 1995] or pre-Silurian.

4.2. Late Paleozoic Ophiolites

[21] Early-middle Devonian radiolaria fossils and coral fossils were found respectively in the cherts and limestone lenses from the Darbut ophiolite melange [*Xiao et al.*, 1991; *Zhang et al.*, 1995]. Sm-Nd dating for the Darbut cumulate rocks mainly the gabbros gives an isochron age of 395 ± 12 Ma [*Zhang et al.*, 1995]. In the Karamaili ophiolite melange, early-middle Devonian microfossils including radiolaria were discovered in the cherts [*Li*, 1995].

[22] U-Pb dating for the zircons from the trondjemite in the Kekesentao-Qiaoxiahala-Kuerti ophiolite belt gives a formation age of 390 Ma [*Chen et al.*, 1997]. Together with middle-late Devonian radiolaria fossils found in the cherts, this ophiolite belt is regarded as formed in the middle-late Devonian [*Chen et al.*, 1997; *He et al.*, 1994].

4.3. Late Devonian-Early Carboniferous Northern Tianshan Ophiolite Belt

[23] The Bayingou ophiolite is a representative and well-preserved ophiolite in this belt. Microfossils including radiolaria and conodont discovered in the cherts from the ophiolite melange suggest its formation age of late Devonian-early Carboniferous [*Xiao et al.*, 1991; *Gao et al.*, 1997; K. Qin, post-doctorial report, 2000].

[24] In general, the Paleozoic ophiolites in the northern Xinjiang occurred as an age pattern of gradual younging from the center to the north and south (Figure 2). If we plot our data into Figure 21.18 of *Şengör and Natal'in* [1996b], the early Paleozoic Tangbale-Mayile-Hongguleleng-Aermantai ophiolite belt could be part of their unit 14, the late Paleozoic Darbut-Karamaili ophiolite belt and the northern Tianshan ophiolite belt be part of unit 15, and the late Paleozoic Kekesentao-Qiaoxiahala-Kuerti ophiolite belt be part of unit 19 (Figure 2).

5. Geochemistry and Origin of the Ophiolites

[25] The geochemistry and origin for these ophiolites were widely discussed elsewhere in the Chinese literature and also in international publications [e.g., *Feng et al.*, 1989]. In this section, we will present a synthesized geochemical review for all the ophiolites, and further constrain their origin (Table 1, data sources are from *Zhang et al.* [1995] and this study). Because of late-stage hydrothermal alteration with different degree extensively occurred during formation and emplacement of these ophiolites [e.g., *Feng et al.*, 1989; *Zhang et al.*, 1995], we will mainly use the immobilized or weakly mobilized elements to determine their magmatic origin.

5.1. Cambrian-Ordovician Tangbale-Hongguleleng-Aermantai Ophiolite Belt

[26] The mantle peridotites from the Tangbale ophiolite are mainly harzburgites, dunites with minor lherzolites. The harzburgites with high Mg# (average Mg# = 100Mg/(Mg + Fe^{total}) = 93) [*Zhang et al.*, 1995] consists of olivine (Fo = 91–92), Cr-spinel and orthopyroxene (En = 90–94) [*Zhu et al.*, 1987], indicative of highly depleted mantle residues. The Cr-spinels have a wide range of Cr# (Cr# = 100Cr/(Cr + Al) = 30–90) and plot in the fields of ophiolitic peridotites from ridge, transitional to arc or more depleted end-sources (Figure 3a). Most of the spinels from the harzburgites and dunites have high Cr# ($\geq$60) and are of the III-type peridotite proposed by *Dick and Bullen* [1984], indicating that the highly depleted mantle peridotites are of arc-related and formed in an environment associated with a subduction zone. The harzburgites and dunites are characterized by low Al_2O_3, CaO and TiO_2 contents [*Zhang et al.*, 1995], suggesting high degrees of partial melting. The cumulate complex is mainly composed of dunite, peridotite, pyroxenite and gabbro. The mafic lavas can be classified into two groups, namely, tholeiites from the mid-ocean ridge basalt (MORB) type and the island arc basalt (IAB) type, respectively, as shown by the Cr-Y and Hf-Th-Ta diagrams (Figures 4 and 5a) and primitive mantle-normalized trace element patterns (Figure 6). The εNd values of the gabbros and basalts are in the range of 7.3–7.9 (Table 2) [*Zhang et al.*, 1995]. In the Sr-Nd diagram, the Tongbale basalts mainly fall in the field of modern Pacific arc systems, and one sample in the MORB field (Figure 7).

[27] The Hongguleleng mantle peridotites are also mainly harzburgites (Mg# = 91). Most of the spinels from the harzburgites plot in the fields of ophiolitic peridotites from ridge and transitional in the Cr#-Mg# diagram (Figure 3a). The cumulate complex is well developed and comprises plagioclase-bearing dunite, troctolite, pyroxenite, olivine gabbro, and gabbro. Some diabase dykes in the cumulate complex are LREE-depleted. The extrusive lavas are mainly MORB-type, transitional and IAB-type tholeiites (Figures 5a and 6). The εNd values of the cumulate rocks and basalts are in the range of 7.2–8.7 (Table 2) [*Zhang et al.*, 1995; *Huang et al.*, 1999]. In the Sr-Nd diagram, one of the Hongguleleng basalts falls in the MORB field, and another displays higher initial Sr value possibly affected by later hydrothermal alteraction (Figure 7).

Table 1. Representative Trace Element (ppm) Contents of the Basalts in the Paleozoic Ophiolites

Sample	Th	Nb	Ta	La	Ce	Pr	Nd	Zr	Sm	Eu	Gd	Ti	Dy	Y	Er	Yb	Lu	Hf	Cr
									Tangbale										
T21	0.32		0.228	1.35	3.79		2.68	36	0.853	0.383		2765				1.3	0.213	0.51	222
T35	0.527		0.231	3.31	7.9		5.19		1.51	0.514		4852				1.18	0.175	1.31	21.6
T40	0.598		0.152	3.21	7.51		5.67		1.61	0.496						1.51	0.231	1.15	26.1
T14-1	0.269		0.16	3.99	10.1		7.78	63.5	2.6	0.813				21.1		2.81	0.437	2.03	84.1
T14-2	0.329		0.315	4.17	10.5		8.97	74.8	3.16	0.987		5870		25.4		2.93	0.448	1.76	78.8
T14-3	0.296		0.319	4.32	10.5		8.35	64.2	2.98	0.968		5810		22.3		2.87	0.434	1.95	71
									Honggguleleng										
H5-5	0.52		0.258	5.95	13.1		9.13	85.1	2.91	1.15		7860				3.08	0.487	2.03	234
H5-10	0.64		0.287	8.8	21.1		13.6	93.1	3.82	1.15		13080				2.9	0.42	3.16	84
H5-8	0.31		0.283	2.71	7.16		5.98	184.1	1.88	0.149						2.21	0.338	2.24	133.3
HC35	1.23		0.223	7.03	15		10.6	104	3.02	0.982		5700				1.82	0.259	2.06	18.4
HC33	1.69		0.104	6.43	15.3		9.27	128	2.73	0.9		4320				2.01	0.29	1.78	134
X-48	1.4		0.287	8.9	17.5		11	108.3	3.09	1.01		4260				1.36	0.217	1.52	289
HM22	2.64		0.383	12.7	29.4		16.8	213	4.27	1.43		12000				2.26	0.309	2.57	118
HM 23	0.328		0.136	3.5	7.92		5.48	131.4	1.78	0.79		10620				2.07	0.32	1.6	221
HM24	0.8		0.627	19.4	39.3		21.8	163	5.58	1.8		11200				2.38	0.329	4.11	699
									Aermantai										
2	0.41	0.586	0.199	3.16	7.127	1.086	5	19.52	1.485	0.462	2.025	3872	2.003	10.74	1.102	1.211	0.208	0.635	26.16
3	1.197	2.465	0.845	5.66	12.57	1.72	6.394	61.46	1.881	0.864	2.551	4331	2.453	13.11	1.551	1.615	0.229	1.636	48.69
6	1.051	1.295	0.5	5.562	11.84	1.651	6.657	41.17	2.26	0.758	2.159	3651	2.747	14.57	1.783	1.641	0.254	1.166	127.1
7	0.808	2.578	0.422	7.188	18.58	2.781	11.91	84.83	3.49	1.447	4.029	7698	3.973	21.68	2.472	2.395	0.393	2.27	192.1
17	0.873	0.893	0.369	6.385	16.09	2.011	10.31	41.4	2.55	0.872	2.538	4035	2.159	10.89	1.251	1.266	0.174	1.329	33.64
19	1.61	1.357	0.221	11.81	27.42	3.363	16.53	55.94	3.885	1.337	3.898	5958	3.537	17.2	1.903	1.641	0.259	1.647	24.81
24	0.406	0.587	0.149	3.835	9.2	1.199	5.955	34.4	1.611	0.575	2.209		2.464	12.61	1.433	1.289	0.243	0.89	50.71
28	5.053	9.468	0.674	25.55	59.6	6.783	28.25	118.1	4.762	1.805	4.762		3.664	18.86	2.097	1.773	0.241	2.719	8.58
8	0.826	6.02	0.265	8.39	19.54	2.89	11.7	50.87	3.336	1.347	4.007		4.26	19.89	2.131	2.151	0.307	1.324	83.83
10	0.685	5.253	0.296	6.234	14.99	2.145	9.235	44.76	2.262	0.982	2.866		3.166	16.33	1.854	1.853	0.262	1.334	258
14	7.513	7.174	0.908	22.89	49.48	5.487	21.56	182.2	4.551	1.693	3.766	3763	3.47	18.34	2.288	2.208	0.312	5.302	21.59
22	0.994	13.99	0.946	10.63	28.97	3.773	17.8	60.42	3.676	1.736	5.084	11597	4.966	24.11	2.783	2.33	0.34	1.976	144.7

Table 1. (continued)

Sample	Th	Nb	Ta	La	Ce	Pr	Nd	Zr	Sm	Eu	Gd	Ti	Dy	Y	Er	Yb	Lu	Hf	Cr
37	8.62	6.243	0.613	24.03	54.06	6.286	23.43	80.54	4.442	1.6	4.857	3886	3.443	15.37	1.532	1.537	0.236	2.075	75.44
38	2.258	3.69	0.326	7.103	17.03	1.975	9.143	67.22	2.48	0.993	2.908		3.407	18.52	2.278	1.74	0.406	1.966	424.5
42	0.442	1.43	0.823	1.773	4.271	0.585	2.421	98.55	0.756	0.459	0.634	1373	0.879	4.37	0.422	0.413	0.076	2.29	114.9
44	0.3	1.655	0.637	3.37	10.84	1.663	7.594	50.77	2.236	1.045	2.836		3.846	18.33	2.081	1.823	0.338	1.59	384.7
									Mayile										
Sb12	0.53		0.277	7.65	19.8		12.7	745	5	1.84		11988				0.89	0.899	1.86	33.8
Sb18	1.43		0.898	12.9	20.6		17.7		5.41	1.92		11388				2.87	0.398	3.43	205
Sb22	0.574		0.57	9.23	24.6		13.6		5.84	2.43		13486				6.86	1.06	2.63	215
HN8	2.67		0.128	17.5	27.4		18	148	4.56	1.34		7250				2.38	0.318		
HN48	4.37		0.744	27	64.1		30.9	172	8.21	2.18		12050				3.43	0.478		
HN18	3.42		0.175	20.1	40.3		21.6	141	4.1	1.23		6050				1.1	0.162		
HN43	1.71		0.373	11.3	25.6		17.3	127	3.81	1.34		7910				2.3	0.274		
									Darbut										
D18-1	0.227		0.363	2.97	8.73		6.08	63.7	2.13	0.758		8985				2.39	0.349	1.41	68.3
D18-5	0.383		0.572	2.28	6.51		5.32	74.1	1.88	0.705						2.16	0.311	1.56	49.8
SJ23	0.215		0.468	3.32	8.7		7.18	66	2.45	0.971		6889		32		2.53	0.343	1.85	270
SJ15	0.229		0.289	3.4	9.51		7.8	62	2.44	0.926		6769		33		2.75	0.362	1.49	300
X20	0.581		0.339	5.73	12.7		9.12	68.9	3.01	1.02		6240		17.6		2.33	0.356		27.7
X100	1.39		1.22	14.5	27.2		17.7	138	4.71	1.45		11760		18.9		2.29	0.315		80.5
X5	5.62		2.97	57.8	83.2		48.2	396	10.8	3.27		13260		42.9		3.33	0.456		53
D19-1	3.99		2.48	28.7	65.1		28	186	7.11	2.36		18300				3.92	0.593		
D19-2	2.71		2.8	27.2	50.9		26.2	192.5	5.6	1.84		14040				3.13	0.489		
									Karamaili (Gabbro)										
K1	0.65	1.19	0.3	16	33.69	4.23	18.77	48.78	3.75	1.19	4.37	6720	4.66	27.9	2.98	2.67	0.4	1.61	25.15
K2	0.52	1.29	0.29	5.71	14.12	2.23	12.18	56.44	3.53	1.36	4.65	7140	4.95	29.43	3.14	2.9	0.45	1.89	26.57
K3	0.41	1.12	0.25	4.56	12.16	2.16	11.84	66.4	3.23	1.31	4	7260	4.45	26.39	2.74	2.76	0.42	2.07	23.05
K4	0.57	1.49	0.29	26.41	55.26	6.75	28.9	58.29	5.05	1.27	5.8	9180	6.61	37.73	4.13	3.76	0.54	2.17	244.9

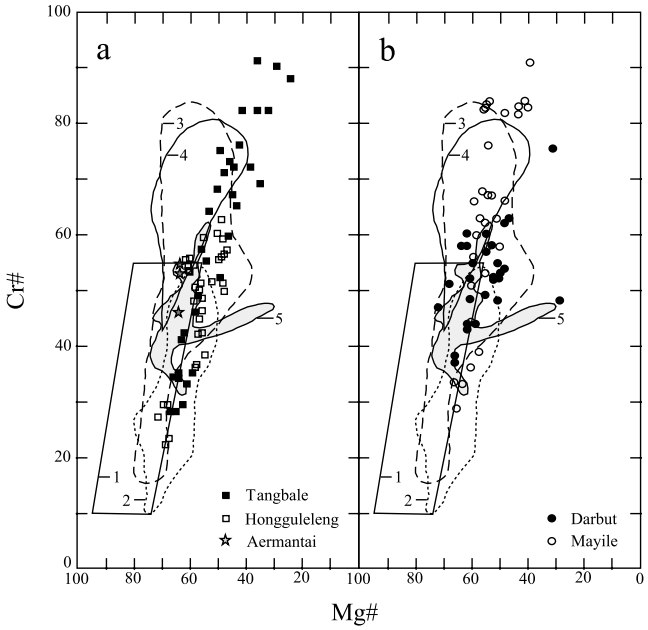


Figure 3. Cr# vs. Mg# diagram for spinels from the mantle peridotites of the Paleozoic ophiolites. 1-field of MORB spinel; 2-field of ophiolitic peridotite spinel from ridge; 3-from transitional; 4-from arc; and 5-from back arc basin (classification of *Dick and Bullen* [1984]).

[28] The mantle peridotites in the Aermantai ophiolite are mainly harzburgites and lherzolite, and consist of olivine (Fo = 90–91), Cr-spinel (Cr# = 45–55) and orthopyroxene (En = 88–90) (Jin et al., unpublished report, 1995), indicative of less depleted mantle residues. The Cr-spinels plot in the field of ophiolitic peridotites from arc or back arc basin (Figure 3a). The cumulate rocks are mainly pyroxenite and gabbro. In the Cr-Y diagram (Figure 4), the lavas plot in the field of IAB, while in the Hf-Th-Nb diagram they mainly plot in the field of IAB and some samples in the field of E-MORB (Figure 5b). In the Ce/Nb-Th/Nb diagram, the lavas

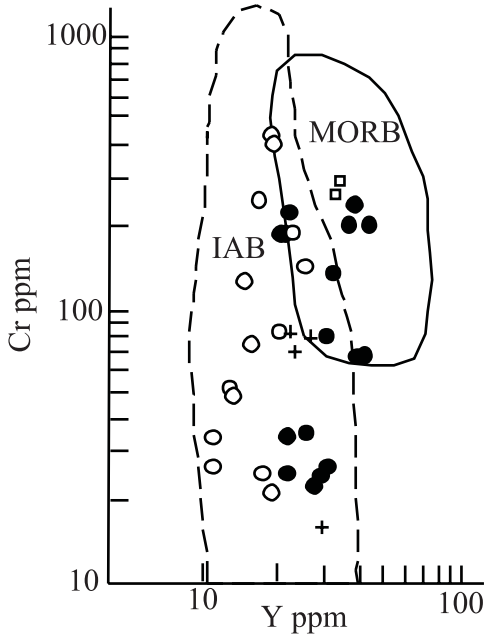


Figure 4. Cr versus Y discrimination diagram for the basalts from the Tangbale ophiolite (crosses), Aermantai ophiolite (open circles), Darbut ophiolite (open squares) and Karamaili ophiolite (solid circles). MORB, mid-ocean-ridge basalt, IAB, island arc basalt.

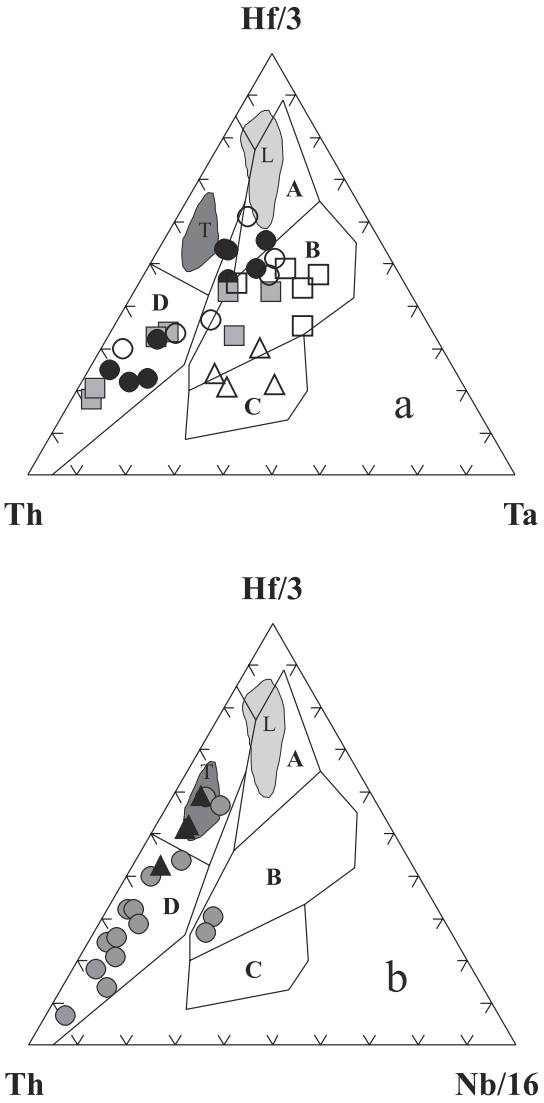


Figure 5. (a) Th-Hf-Ta discrimination diagram for the basalts from the Tangbale ophiolite (open circles), Hongguleleng ophiolite (solid circles), Mayila ophiolite (solid squares) and Darbut ophiolite (open squares for E-MORB type, open triangles for OIB-type). (b) Th-Hf-Nb discrimination diagram for the basalts from the Aermantai ophiolite (solid circles), and for the gabbros from the Karamaili ophiolite (solid triangles). A, N-MORB, B, E-MORB, C, OIB (ocean island basalt); D, IAB. Data for fields of the Tofua arc (T) and Lau back arc basin (L) are from *Hawkins* [1995].

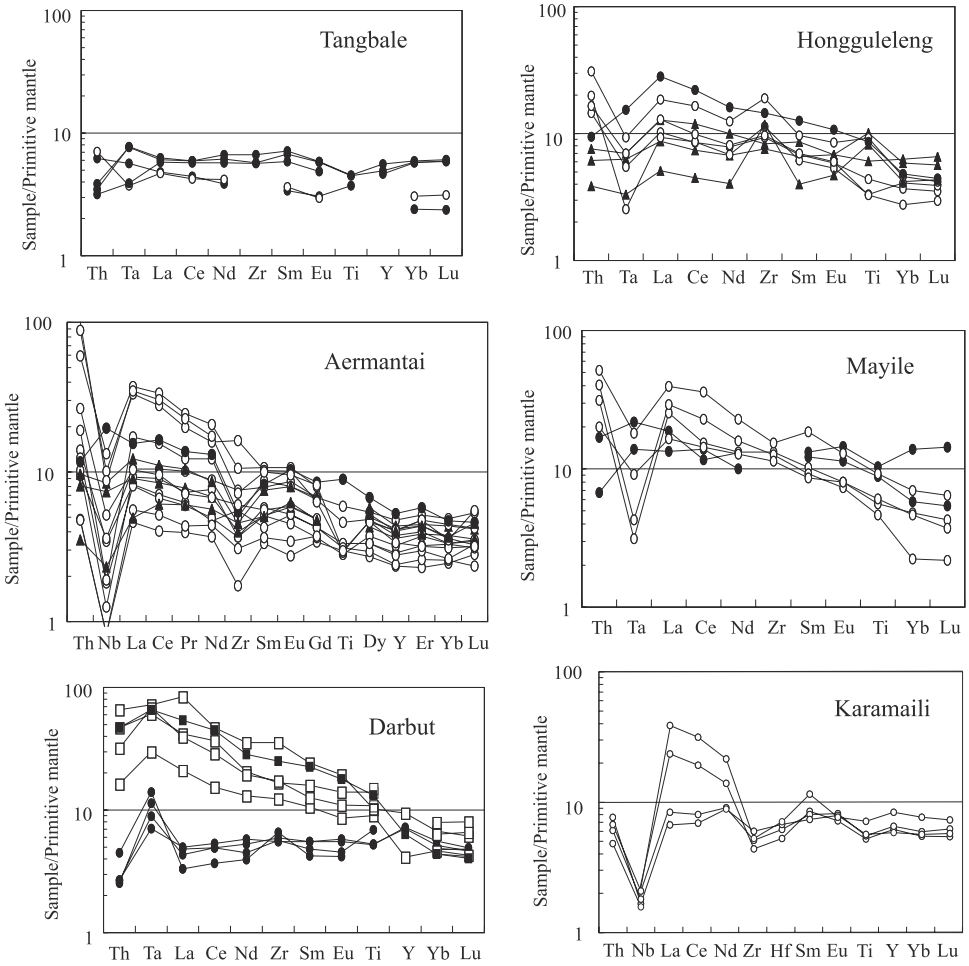


Figure 6. Primitive mantle-normalized trace element patterns for the basalts and gabbros (Karamaili) from the Paleozoic ophiolites. The patterns with obvious Nb(Ta) negative anomalies and variable LREE-enrichment represent the IAB-type basalts (open circles), those with no or slight negative Nb(Ta) anomalies represent the IAB-MORB transitional basalts (solid triangles), and those with distinguishable Nb(Ta) positive anomalies and flat to LREE-depletion represent the MORB-type basalts (solid circles). OIB-type basalts are shown in the Darbut patterns (open squares), and typical OIB also shown for comparison (solid square). Normalizing values and data source for typical OIB are from *Sun and McDonough* [1989].

range from E-MORB, transitional to IAB (not shown), consistent with their trace element patterns (Figure 6). The εNd values of the basalts are in the range of 5.4–6.3 (Table 2), and in the Sr-Nd diagram, the basalts mainly fall in the field of modern Pacific arc systems (Figure 7).

5.2. Silurian or Pre-Silurian Mayile Ophiolite

[29] The Mayile mantle peridotites are mainly harzburgites (Mg# = 92) with minor dunites and lherzolites. The Cr-spinels have a wide range of Cr# (30–90) and mostly plot the fields of ophiolitic peridotites from ridge, transitional to arc or more depleted end-sources, comparable to those of the Tongbale ophiolite. The cumulate complex is well developed and comprises clinopyroxene peridotite, olivine pyroxenite, pyroxenite, gabbro and plagiogranite. The mafic lavas can be classified two groups, namely MORB-type and IAB-type tholeiites, respectively, as shown by the Hf-Th-Ta diagram (Figure 5a) and primitive mantle-normalized trace element patterns (Figure 6). The geochemistry of the ophiolite is strikingly similar to that of the Tongbale ophiolite, arguably suggesting close petrogenic relationship between the two ophiolites.

5.3. Early-Middle Devonian Darbut-Karamaili Ophiolite Belt

[30] The mantle peridotites in the Darbut are mainly harzburgites (Mg# = 92) with minor dunites and lherzolites, and their Cr-spinels mostly plot in the fields of ophiolitic peridotites from ridge to transitional settings (Figure 3b). The cumulate complex is mainly composed

Table 2. Representative Sr-Nd Isotopic Analyses for the Basalts in the Paleozoic Ophiolites[a]

Sample	Sm	Nd	$^{147}Sm/^{144}Nd$	$^{143}Nd/^{144}Nd$	εNd(t)	Rb	Sr	$^{87}Rb/^{86}Sr$	$^{87}Sr/^{86}Sr$	$^{87}Sr/^{86}Sr(I)$
				Hongguleleng (t = 444 Ma)						
H-5-2	3.641	24.31	0.1495	0.51287	7.2	12.25	332.6	0.03682	0.70344	0.70321
H-5-5	3.152	16.05	0.1964	0.51306	8.15	6.933	302.1	0.02295	0.7047	0.70455
				Tangbale (t = 500 Ma)						
TB-37	3.123	23.11	0.1351	0.51284	7.89	67.07	297.8	0.2252	0.70553	0.70393
TB-76	2.482	17.94	0.1384	0.51284	7.68	47.52	245.4	0.1352	0.70462	0.70365
T-4-1	3.603	17.54	0.2054	0.51304	7.34	70.82	136.1	0.5205	0.70702	0.70331
T-6-1	2.869	18.82	0.1524	0.51288	7.47	53.24	146.1	0.3644	0.70555	0.70295
				Aermantai (t = 480 Ma)						
XJ-2	1.481	8.247	0.1798	0.51288	5.74	59.71	1150	0.0519	0.70457	0.70421
XJ-3	1.912	12.06	0.1586	0.51282	5.93	152	106.7	0.2217	0.7055	0.70398
XJ-6	1.916	11.43	0.1676	0.51287	6.29	86.69	552.1	0.157	0.70549	0.70441
XJ-8	3.0	18.46	0.1625	0.51284	5.96	134.4	455	0.2953	0.7059	0.70388
XJ-14	4.306	36.23	0.1189	0.51267	5.4	20.48	380.1	0.05387	0.70468	0.70431
XJ-17	2.451	16.74	0.1464	0.51277	5.72	46.1	235.4	0.1959	0.70554	0.7042
XJ-19	3.938	27.02	0.1458	0.51276	5.52	44.07	270.2	0.1631	0.70547	0.70436
XJ-20	4.387	30.21	0.1452	0.51277	5.71	5.327	638.5	0.00834	0.70411	0.70406
				Darbut (t = 395 Ma)						
SJ-15	2.256	11.21	0.2012	0.5129	4.9	31.89	172.8	0.1846	0.70684	0.7058
SJ23	2.357	11.04	0.2135	0.51295	5.3	4.059	167.5	0.02577	0.7062	0.70605
SF55	2.433	11.91	0.2041	0.51293	5.36	4.248	156.4	0.08849	0.70567	0.70517

[a]The data of Rb-Sr and Sm-Nd analyses are from *Zhang et al.* [1995] and *Huang et al.* [1997]. We recalculate the initial Sr and Nd values using the age data discussed in the text.

of troctolite and gabbro. In the Hf-Th-Ta diagram (Figure 5a), the Darbut extrusive rocks clearly display two groups of magma suites, i.e., E-MORB tholeiites (also shown by Cr-Y diagram, Figure 4) and ocean island basalts (OIB) respectively, consistent with their primitive mantle-normalized trace element patterns (Figure 6). The εNd values of the cumulate rocks are 7.5–9.0 [*Zhang et al.*, 1995], and the values of the tholeiites are 4.9–5.4 (Table 2). In the Sr-Nd diagram, the tholeiites do not plot in any comparison field (Figure 7), possibly indicating that they had been affected by EMII-type OIB magma sources. This effect is also shown by clear positive Ta anomaly on the primitive mantle-normalized trace element variation diagrams, since positive Ta and Nb anomalies are normally and typically related to OIB magmas.

[31] The Karamaili ophiolite is mainly composed of harzburgites, gabbros, diabases and basalts. The gabbros display arc tholeiite affinity as shown in the diagrams of Hf-Th-Nb (Figure 5b) and Ce/Nb-Th/Nb (not shown), and their trace element patterns with obvious negative Nb anomaly and flat to LREE-enrichment (Figure 6). In the Cr-Y diagram (Figure 4), the extrusive rocks plot in the fields of IAB and MORB.

5.4. Middle-Late Devonian Kekesentao-Qiaoxiahala-Kuerti Ophiolite Belt

[32] Because of lack of detailed geochemical data, the petrogenesis of this ophiolite belt is poorly constrained. Previous studies indicate that the ophiolite mainly comprises lherzolites and MORB-type basalts [*Chen et al.*, 1997]. Boninitic-like or high Mg volcanics, which characterized by enriched in Si and Mg, and depleted in Ti and other HFSE, were discovered in the middle Devonian ophiolite-associated assemblages [*Liu and Zhang*, 1993;

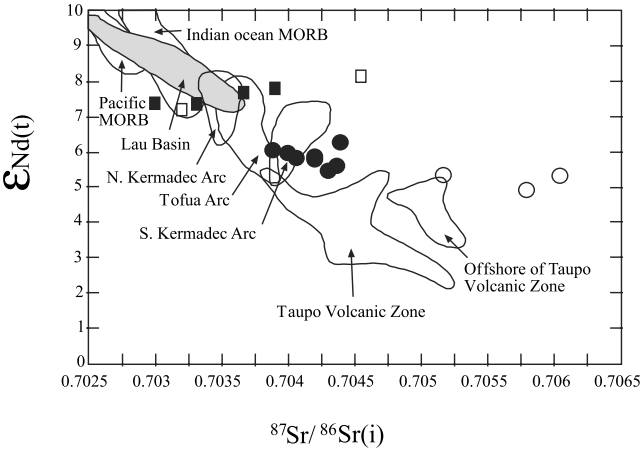


Figure 7. Sr-Nd isotope covariation diagram for the basalts from the Tangbale ophiolite (solid squares), Hongguleleng ophiolite (open squares), Aermantai ophiolite (solid circles) and Darbut ophiolite (open circles). Fields for Pacific MORB, Indian ocean MORB, Lau basin basalts, Tofua arc lavas, northern and southern Kermadec arc basalts, Taupo volcanic zone and Offshore basalts are from *Ito et al.* [1987], *Klein et al.* [1991], *Hergt and Hawkesworth* [1994] and *Gamble and Wright* [1995].

He et al., 1994; *Liu et al.*, 1999] (Figure 2). Furthermore, adakitic-like volcanic rocks were recently recognized from the early Devonian ophiolite-associated arc volcanics [*Xu et al.*, 2001] (Figure 2). These rocks share lots of common geochemical characters with modern adakites, like high in Si, Mg, Al and Sr, and poor in Y, Yb and HREE [*Xu et al.*, 2001].

5.5. Late Devonian-Early Carboniferous Northern Tianshan Ophiolite Belt

[33] The representative Bayingou ophiolite in this belt was commonly regarded as a part of the Tianshan orogenic belt [e.g., *Windly et al.*, 1990; *Allen et al.*, 1992; *Chen et al.*, 1999], whereas tectonically also related to evolution of the ophiolites in the Junggar region [e.g., *Allen et al.*, 1992]. The ophiolite is mainly composed of mantle peridotites, gabbros and basalts. The basalts can be classified into three groups of magma suites, MORB-type (LREE-depleted and moderate Ti), IAB-type (slightly LREE-enriched and depleted in Yb, Zr and other HFSE) and OIB-type (highly fractionated LREE and HREE, and enriched in Ti, P and K), respectively [*Zhang and Zhou*, 2001].

6. Petrogenesis of the Associated Assemblages

6.1. Paleozoic Sedimentary Sequences

[34] As presented in section 3, the Paleozoic ophiolite-associated sedimentary sequences are mainly composed of volcanoclastic rocks, cherts, flysch and some lenses of limestones. The cherts commonly bear radiolaria fossils, which generally used to constrain the formation ages of the ophiolites. Major element geochemistry of the cherts suggests that they deposited near related oceanic spreading ridges [*Zhang et al.*, 1995]. The main components in the volcanoclastic rocks are less fractionated, and are composed of feldspar, quartz, and detritals of andesite, dacite, basalt and tuff, together with some minerals of biobite, olivine, pryoxene and amphibole. Their grain parameters are comparable to typical sediments from the andesite-dacite island arcs. Major and trace element geochemistry [*Wu et al.*, 1993; *Zhang et al.*, 1995] documents that they are pelagic-abyssal sediments deposited in a major ocean, and that their sources were closely related to island arcs, namely oceanic island arcs in the early Paleozoic (Ordovician and Silurian) and marginal island arcs in the late Paleozoic (Devonian and Carboniferous), indicating an evolution history from intraoceanic to marginal settings, also as suggested by *Şengör and Natal'in* [1996a, 1996b].

6.2. Subduction-Related Paleozoic Magmatism

[35] Andesites, diorites and granitoids widely developed and closely associated with the respective ophiolite in spatial and temporal. The diorites and granitoids plot in the volcanic arc field in the diagrams of Yb+Ta-Rb and Yb-Ta, and the andesites have indistinguishable REE patterns with the rocks from typical island arcs [*Zhang et al.*, 1995]. Pb-Pb isotopic data of the granitoids show a clear maturing trend from the early Paleozoic ones to the late Paleozoic ones [*Li*, 1991], also suggesting that these subduction-related magmatisms evolved from intraoceanic settings to marginal settings.

6.3. Postorogenic Late Carboniferous-Permian Granitoids

[36] U-Pb dating for zircons from the post-orogenic granitoids and Rb-Sr dating for the whole-rock samples suggest that magma of these rocks crystallized in 320–250 Ma [*Kwon et al.*, 1989; *Wang et al.*, 1993]. Initial Pb isotope ratios determined for these rocks show clear affinity with ratios from mid-ocean ridge basalts in Pb isotope correlation diagrams [*Kwon et al.*, 1989; *Jin and Zhang*, 1993]. Sr-Nd isotopic studies indicate that the granitoids have low initial Sr (0.7047–0.7051) and high initial Nd (2.1–5.1) values [*Kwon et al.*, 1989; *Wang et al.*, 1993; *Wu et al.*, 1997], also indicative of clear oceanic affinity. Therefore the magma sources for the post-orogenic granitoids are large ion lithophile element-depleted material of oceanic affinity, arguably the accreted complexes of the aforementioned Paleozoic ophiolites and associated assemblages [e.g., *Feng et al.*, 1989].

[37] Furthermore, the young model ages and high initial Nd values of the post-orogenic granitoids support the idea that the Junggar region is composed of young accreted oceanic and island arc assemblages, with no involvement of old crust. And the Junggar basin itself could be based by orogenically deformed Altaid Paleozoic rocks [*Suess*, 1901; *Argand*, 1924; *Ren et al.*, 1987; *Zhang et al.*, 1993; *Şengör et al.*, 1993; *Allen et al.*, 1995; *Şengör and Natal'in*, 1996a, 1996b].

7. Paleozoic Tectonic Evolution of the Northern Xinjiang

[38] The presented geologic, geochronologic and geochemical data suggest that the Paleozoic geology of the northern Xinjiang is characterized by numerous ophiolite belts closely associated with island arc rocks and abyssal deposits, the paucity of ancient gneiss terranes representing former continental fragments, and enormous crust accretion. The Paleozoic ophiolites and associated assemblages of the western and eastern Junggar regions are tectonically (spatial and temporal) related, permitting us to reconstruct the Paleozoic tectonic framework and evolution for the northern Xinjiang, using a subduction-accretion model as proposed by A. M. C. Şengör and others for interpreting evolution of the entire Altaids [*Şengör et al.*, 1993; *Şengör and Natal'in*, 1996a, 1996b]. We here adopt this model rather than other competing models (such as archipelago model) mainly due to the consideration that, the extrusive rocks in the Paleozoic ophiolites are mainly MORB-, OIB- and IAB-type basalts (section 5). No typical BABB (back arc basin basalt) is recognized from the available geochemical data. Some transitional basalts in the Honggule-leng and Aermantai ophiolites have similar characteristics to the BABB, like Nb(Ta) troughs and flat REE signatures

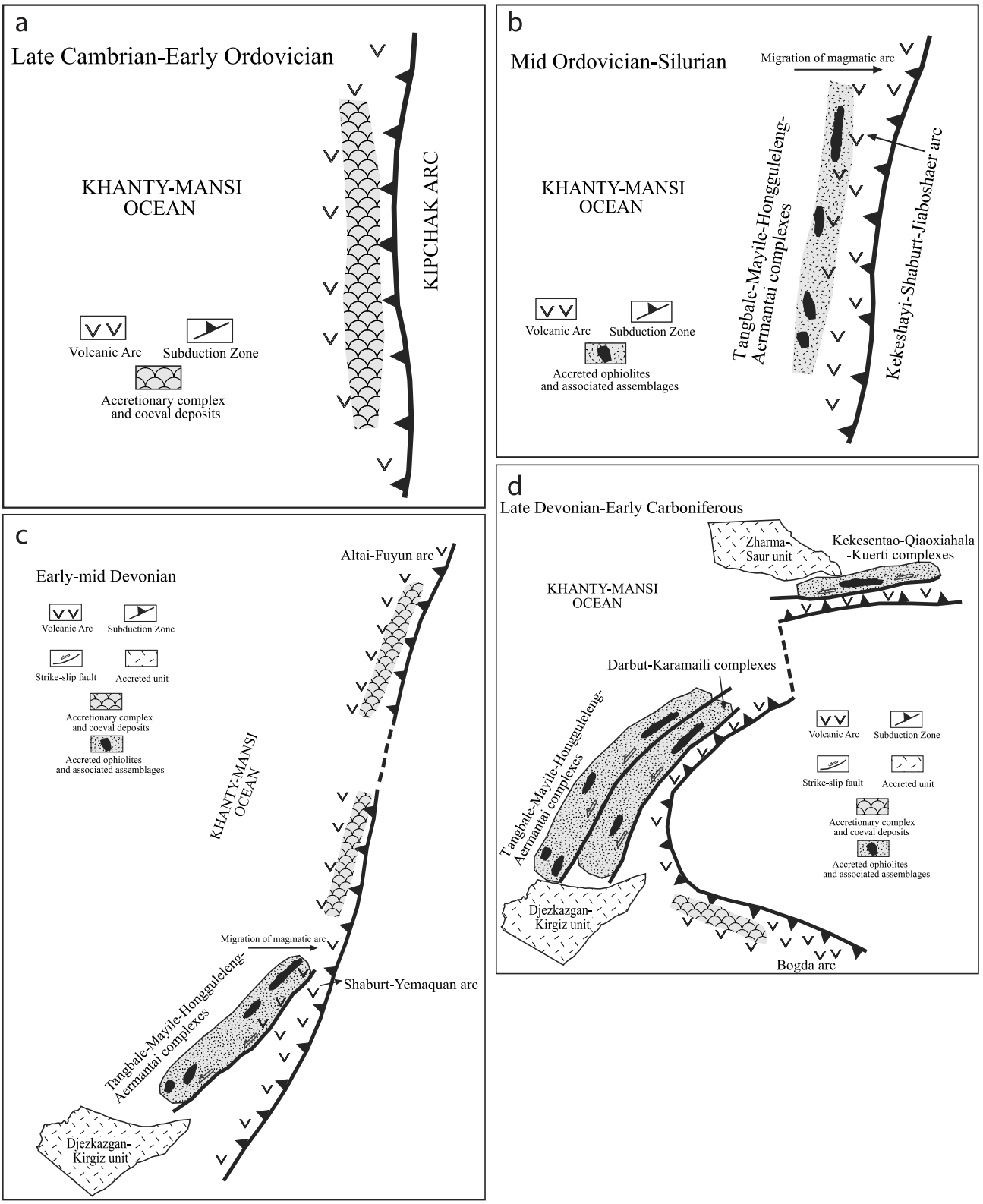


Figure 8. (a–e) Schematic map-view diagrams illustrating tectonic evolution the northern Xinjiang in the Paleozoic, using a model of subduction-accretion and large-scale map view strike-slip faulting. See text for detailed discussion.

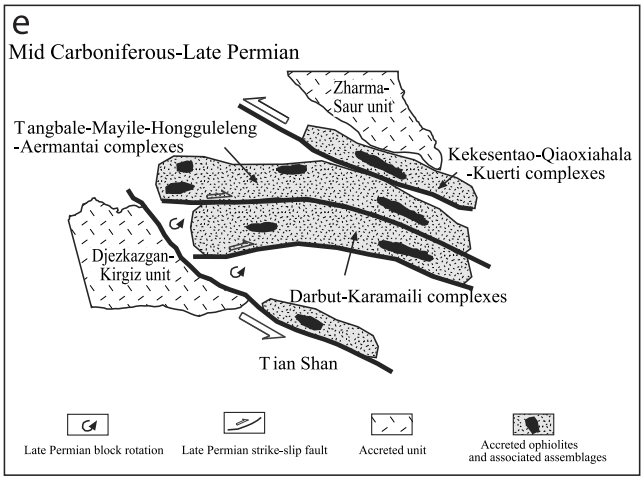


Figure 8. (continued)

(Figure 6). Whether these basalts erupted in back arc basin settings or not still requires further research.

7.1. Early Paleozoic Subduction-Accretion

[39] Former discussion has excluded any Precambrian continental blocks involving the accretion of the region, and multiple collisions of some microcontinental blocks or terranes. This implies that the tectonic evolution of the region mainly occurred in an oceanic setting, and in this area the Khanty-Mansi ocean behind the Kipchak Arc (Figure 8a) [see also *Şengör and Natal'in*, 1996b, Figures 21.30–32]. Oceanic subduction in the late Cambrian-early Ordovician produced basaltic to andesitic volcanic rocks, and in front of them there were coeval arc-related deposits and accretionary oceanic fragments composed of the Cambrian-Ordovician ophiolites and abyssal sediments, originally in a near north-south trend (Figure 8a). The early Ordovician blueschists in the Tangbale ophiolite melange (Figure 2) indicates high-pressure metamorphism resulted from subduction of ocean crust [e.g., *Coleman*, 1989]. The Tangbale-Hongguleleng-Aermantai complexes possibly accreted together at the end of the early Ordovician.

[40] Migration of magmatic arc towards the subduction zone produced a chain of intraoceanic island arcs, the middle-late Ordovician-Silurian Kekeshayi-Shaburt-Jiaboshaer complexes of andesitic volcanic and volcanoclastic rocks, which imposed upon the Ordovician Tangbale-Hongguleleng-Aermantai subduction-accretion complexes (Figure 8b). Flysch and other abyssal sediments unconformably deposited upon the Ordovician ophiolites. The Mayile ophiolite was also accreted to the Ordovician complexes at this time (Figure 8b). No evidence shows that the early Paleozoic subduction-accretion process resulted in any closure of oceans and any collision between continental blocks. The accreted early Paleozoic complexes are mostly covered by the Devonian-Carboniferous rocks (Figure 1).

7.2. Late Paleozoic Subduction-Accretion

[41] Oceanic subduction together with migration of magmatic arc in the early-mid Devonian produced a chain of oceanic island arcs represented by the Devonian Shaburt-Yemaquan complexes (Figure 8c), which imposed upon part of the early Paleozoic complexes like at the Hongguleleng and Aermantai areas. While at the Mayile and Tangbale areas, the early Paleozoic complexes are unconformably covered by clastic sediments and marine flysch with silicic pyroclastics of mid-Devonian, and not affected by any volcanism. The geological difference along the trend of the early Paleozoic complexes in the early-mid Devonian possibly resulted from strike-slip faulting, which transferred the southern part of the complexes away from the subduction zone and towards other accreted Altaid unit (Djezkazgan-Kirgiz unit [*Şengör and Natal'in*, 1996b]) (Figure 8c). The early-middle Devonian Darbut-Karamaili ophiolites and the contemporary island arc rocks and abyssal sediments (Figure 8c), plus some off-axis seamount materials (the OIB in the Darbut ophiolite) were accreted to form the late Paleozoic Darbut-Karamaili subduction-accretion complexes in the late Devonian (Figure 8d).

[42] To the north, oceanic subduction also produced the Altai-Fuyun island arc containing the early Devonian adakites and the middle Devonian boninitic-like or high Mg volcanics, which in origin possibly related to forearc extension (Figure 8c). These arc rocks and the middle-late Devonian Kekesentao-Qiaoxiahala-Kuerti ophiolites accreted to form part of unit 19 of *Şengör and Natal'in* [1996b], which transferred from the north by large-scale strike-slip faulting [see *Şengör and Natal'in*, 1996b, Figures 21.35–38].

[43] At the end of Devonian, part of early Paleozoic ophiolite complexes (i.e., the Tangbale ophiolite complex) accreted onto the Djezkazgan-Kirgiz unit following continued strike-slip faulting (Figure 8d) [see also *Şengör and Natal'in*, 1996b, Figures 21.35–36]. $^{40}Ar/^{39}Ar$ dating for amphibole from the amphibolite sole suggests that this accretion happened in 356 Ma (end of Devonian) [*Zhang et al.*, 1995]. Simultaneously, the middle-late Devonian Kekesentao-Qiaoxiahala-Kuerti complexes accreted with the Zharma-Saur unit to the north (Figure 8d). As a consequence, the geological evolution changed from intraoceanic settings to marginal settings, also as documented by aforementioned Paleozoic ophiolite-associated sedimentary sequences and subduction-related magmatisms.

7.3. Late Devonian-Early Carboniferous Subduction-Accretion in the Northern Tianshan

[44] The northern Junggar region mainly deposited interfingered marine and continental sediments with local occurrence of coal horizons during the late Devonian-Carboniferous. Whereas in northern Tianshan, oceanic subduction produced the late Devonian-early Carboniferous island arc rocks (Figure 8d). The Carboniferous Bogda island arc is nucleated by mafic-ultramafic complexes and large doleritic hypabyssal dike and sill complexes [*He et al.*, 1994]. This arc and the Bayingou ophiolite accreted together in the Carboniferous to form the northern Tianshan subduction-accretion complexes as part of unit 15 of *Şengör and Natal'in* [1996b]. And later, a late Carboniferous-early Permian collision accreted the northern side of the central

Tianshan to the northern Tianshan complexes (Figure 8e). This collision is bracketed by the middle Carboniferous termination of arc magmatism and the appearance of late Carboniferous or early Permian clastics in a foreland basin [*Allen et al.*, 1992].

7.4. Postsubduction-Accretion Accommodation

[45] Subduction-accretion processes terminated following elimination of all oceanic floor in the mid-Carboniferous in this region (Figure 8e). Late Carboniferous-Permian post-orogenic granitoids, whose magma sources were the accreted Paleozoic complexes, widely intruded into this region, indicating vertical crust accretion or transfer.

[46] The present configuration of the Paleozoic subduction-accretion complexes is possibly resulted from late Permian-early Triassic accommodation, as suggested by *Allen et al.* [1995]. The Paleozoic complexes in the northern Xinjiang have similar orientation with the rest of the Paleozoic Altaids tectonic units in the mid-Carboniferous. A counterclockwise rotation of fault blocks in the late Permian-early Triassic, with respect to north and south neighboring regions and associated with a giant transtensional (sinistral strike-slip and extension) zone between Altay and Tianshan (Figure 8e), extensively affected the western Junggar accretionary belts and subsequently generated their present configuration. Whereas the configuration of the eastern Junggar accretionary belts remained nearly unchanged in this event [see *Allen et al.*, 1995, Figure 4].

8. Concluding Remarks

[47] Available geochemical data from the Paleozoic ophiolites of the northern Xinjiang, China, indicate that these ophiolites are mainly MORB-, OIB- and IAB-type oceanic fragments with no typical back arc signatures. Together with geologic and geochronologic data, we suggest that the Paleozoic ophiolites and associated assemblages of the western and eastern Junggar regions are tectonically (spatial and temporal) related. Our reconstruction for the Paleozoic tectonic framework and evolution for the northern Xinjiang is of emphasis on growth of subduction-accretion complexes and large-scale map-view strike-slip faulting, largely following the model of A. M. C. Şengör and others for interpreting evolution of the entire Altaids [*Şengör et al.*, 1993; *Şengör and Natal'in*, 1996a, 1996b]. This reconstruction is appropriate for the data presented in this paper, and compatible with the rest of the Altaids. However, detailed palaeomagnetic and structural data are adequately required to further constrain the palaeopositions of the Paleozoic complexes, and their displacements along the boundary faults during and post subduction-accretion processes in this region.

[48] **Acknowledgments.** We thank A. M. C. Şengör for thorough and thoughtful comments, which greatly improved our original interpretation of tectonic evolution. We are also grateful to Brian Wernicke for considerate review. This research was supported by the National 973 Project (2001CB409801), 305 Project and the National Natural Science Foundation of China (49973004).

References

Allen, M. B., B. F. Windley, and C. Zhang, Paleozoic collisional tectonics and magmatism of the Chinese Tien Sahn, central Asia, *Tectonophysics*, *220*, 89–115, 1992.

Allen, M. B., A. M. C. Şengör, and B. A. Natal'in, Junggar, Turfan and Alakol basins as late Permian to? early Triassic extensional structures in a sinistral shear zone in the Altaid orogenic collage, Central Asia, *J. Geol. Soc. London*, *152*, 327–338, 1995.

Argand, E., La Tectonique de I'Asie, *Int. Geol. Congr.*, *13th*, 171–372, 1924.

Bai, W. J., Y. Q. Ren, and S. R. Wang, Petrology, mineralogy and origin of chromite of the Hongguleleng ophiolite, Xinjiang (in Chinese with English abstract), *Bull. Xi'an Inst. Geol. Miner. Resour. Chin. Acda. Geol. Sci.*, *14*, 1–60, 1986.

Chen, C. Y., H. F. Lu, D. Jia, D. S. Cai, and S. M. Wu, Closing history of the southern Tianshan oceanic basin, western China: An oblique collision orogeny, *Tectonophysics*, *302*, 23–40, 1999.

Chen, J. F., T. X. Zhou, Z. Xie, X. Zhang, and X. S. Guo, Formation of positive Nd(T) granitoids from the Alataw Mountains, Xinjiang, China, by mixing and fractional crystallization: Implication for Phanerozoic crustal growth, *Tectonophysics*, *328*, 53–67, 2000.

Chen, Z. F., S. D. Chen, and Y. H. Liang, Opening-closing tectonics of Xinjiang and mineralization (in Chinese with English abstract), Xinjiang Technol. and Sanitation Press, Urumchi, 1997.

Coleman, R. G., Continental growth of northwest China, *Tectonics*, *8*, 621–635, 1989.

Dick, H. J. B., and T. Bullen, Chromian spinel as a petrogenetic indicator in abyssal and alpine-type peridotites and spatially associated lavas, *Contrib. Mineral. Petrol.*, *86*, 54–76, 1984.

Feng, Y., R. G. Coleman, G. Tilton, and X. Xiao, Tectonic evolution of the west Junggar region, Xinjiang, China, *Tectonics*, *8*, 729–752, 1989.

Gamble, J. A., and I. C. Wright, The southern Havre trough: Geological structure and magma petrogenesis of an active backarc rift complex, in *Backarc Basins: Tectonics and Magmatism*, edited by B. Taylor, pp. 29–62, Plenum, New York, 1995.

Gao, J., G. Q. He, and M. S. Li, Paleozoic tectonic evolution of the west Tianshan orogenic belt (in Chinese with English abstract), *Earth Sci.*, *22*, 27–32, 1997.

Hawkins, J. W., The geology of the Lau Basin,in *Backarc Basins: Tectonics and Magmatism*, edited by B. Taylor, pp. 63–138, Plenum, New York, 1995.

He, G. Q., M. S. Li, D. Q. Liu, Y. L. Tang, and R. H. Zhou, *Paleozoic Crustal Evolution and Mineralization in Xinjiang of China* (in Chinese with English abstract), 437 pp., Xinjiang People's Publ. House (Urumchi), Educ. and Cult. Press LTD, Hong Kong, 1994.

Hergt, J. M., and C. J. Hawkesworth, The Pb, Sr, and Nd isotopic evolution of the Lau Basin: Implications for mantle dynamics during backarc opening, *Proc. Ocean Drill. Program Sci. Results*, *135*, 505–517, 1994.

Hsu, K. J., Relic back-arc basins of China and their petroleum potential, in *New Perspectives in Basin Analysis*, edited by K. Kleinspehn, pp. 245–263, Springer-Verlag, New York, 1988.

Hu, A. Q., B.-M. Jahn, G. X. Zhang, Y. B. Chen, and Q. F. Zhang, Crustal evolution and Phanerozoic crustal growth in northern Xinjiang: Nd isotopic evidence: part I. Isotopic characterization of basement rocks, *Tectonophysics*, *328*, 15–51, 2000.

Huang, J. H., Z. D. Jin, and F. C. Li, Sm-Nd isotopes and age of the Hongguleleng ophiolite, *Chin. Sci. Bull.*, *44*, 1004–1007, 1999.

Huang, X., C. W. Jin, B. S. Sun, P. Jun, and R. H. Zhang, Study on the age of Aermantai ophiolite, Xinjiang by Nd-Sr isotope geology (in Chinese with English abstract), *Acta Pet. Sin.*, *13*, 85–91, 1997.

Ito, E., W. M. White, and C. Copel, The O, Sr, Nd, and Pb isotope composition of MORB, *Chem. Geol.*, *62*, 157–176, 1987.

Jahn, B.-M., W. L. Griffin, and B. Windley, Continental growth in the Phanerozoic: Evidence from Central Asia, *Tectonophysics*, *328*, vii–x, 2000.

Jin, C. W., and X. Q. Zhang, Ages and origin of the granitoids in the west Junggar region of Xinjiang (in Chinese with English abstract), *Sci. Geol. Sin.*, *28*, 28–36, 1993.

Klein, E. M., C. H. Langmuir, and H. Staudigel, Geochemistry of basalts from the southeast Indian Ridge, *J. Geophys. Res.*, *96*, 8089–8115, 1991.

Kwon, S. T., G. R. Tilton, R. G. Coleman, and Y. Feng, Isotopic studies bearing on the tectonics of the west Junggar region, Xinjiang, China, *Tectonics*, *8*, 719–727, 1989.

Li, H., Z. C. Gong, X. Y. Dong, and J. T. Zeng, On the geological setting of basic and ultrabasic rocks and the characteristics of regional metallization in the west Junggar of Xinjiang, China (in Chinese with English abstract), *Bull. Xi'an Inst. Geol. Mineral Resour. Chin. Acda. Geol. Sci.*, *18*, 1–140, 1987.

Li, J. Y., On evolution of Paleozoic plate tectonics of east Junggar, Xinjiang, China, in *On Tectonic Evolution of the Southern Margin of the Paleozoic Composite Megasuture Zone* (in Chinese with English abstract), edited by X. C. Xiao and Y. Q. Tang, pp. 92–108, Beijing Technol. Press, Beijing, 1991.

Li, J. Y., Main characteristics and emplacement processes of the east Junggar ophiolites, Xinjiang, China (in Chinese with English abstract), *Acta Pet. Sin.*, *11*, supplement, 73–84, 1995.

Li, J. Y., X. C. Xiao, Y. Q. Tang, M. Zhao, B. Q. Zhu, and Y. M. Feng, Main characteristics of late Paleozoic plate tectonics in the southern part of east Junggar, Xinjiang (in Chinese with English abstract), *Geol. Rev.*, *36*, 305–316, 1990.

Li, Z. X., Tectonic history of the major East Asian lithospheric blocks since the mid-Proterozoic-a synthesis,in *Mantle Dynamics and Plate Interactions in East Asia*, *Geodyn. Ser.*, vol. 27, edited by M. F. J. Flower et al., pp. 221–242, AGU, Washington, D. C., 1998.

Liu, H. C., J. F. Xu, Y. Y. Yu, F. R. Chen, and Z. P. Zheng, High-Mg volcanics and its geological significance from the Altai, Xinjiang, *Chin. Sci. Bull.*, *44*, 1002–1004, 1999.

Liu, W. and X. B. Zhang,The characteristics and geological significance of Ulungur-Zhaisangpo tectonic melange belt, in *New Improvement of Solid Geosciences in Northern Xinjiang* (in Chinese), edited by G. Z. Tu, pp. 217–228, Sci. Press, Beijing, 1993.

Ren, J., C. Jiang, Z. Zhang, and D. Qin, *Geotectonic Evolution of China*, Springer-Verlag, New York, 1987.

Şengör, A. M. C., and B. A. Natal'in, Turkic-type orogeny and its role in the making of the continental crust, *Annu. Rev. Earth Planet. Sci.*, *24*, 263–337, 1996a.

Şengör, A. M. C., and B. A. Natal'in, Paleotectonics of Asia: Fragments of a synthesis, in *The Tectonic Evolution of Asia*, edited by An Yin and T. M. Harrison, pp. 486–640, Cambridge Univ. Press, New York, 1996b.

Şengör, A. M. C., B. A. Natal'in, and V. S. Burtman, Evolution of the Altaid tectonic collage and Paleozoic crustal growth in Eurasia, *Nature*, *363*, 299–307, 1993.

Suess, E., *Das Antlitz der Erde*, Tempsky, Wien, 1901.

Sun, S.-S., and W. F. McDonough, Chemical and isotopic systematics of oceanic basalts: Implications for mantle composition and processes, in *Magmatism in the Ocean Basins*, edited by A. D. Saunders, and M. J. Norry, *Geol. Soc. Spec. Publ.*, *42*, 313–345, 1989.

Tilton, G. R., S. T. Kwon, R. G. Coleman, and X. Xiao, Isotopic studies from the west Junggar Mts., NW Chian, *Geol. Soc. Am. Abstr. Programs*, *18*, 773, 1986.

Wang, G. R., S. D. Cheng, S. D. Yang, Z. M. Zhang, and Y. S. Ou, Map of tectonism-formation in the northern Xinjiang China and its neighboring area (1:1,500,000), China Univ. of Geosci. Press, Beijing, 1995.

Wang, Z. G., Z. H. Zhao, T. R. Zou, and B. Q. Wu, The genetic types of granitoids and their mineralization in northern Xinjiang, in *New Improvement of Solid Geosciences in Northern Xinjiang* (in Chinese), edited by G. Z. Tu, pp. 127–136, Sci. Press, Beijing, 1993.

Windly, B. F., M. B. Allen, C. Zhang, Z. Y. Zhao, and G. R. Wang, Paleozoic accretion and Cenozoic redeformation of the Chinese Tien Shan range, *Central Asia, Geology*, *18*, 128–131, 1990.

Wu, F. Y., B. M. Jahn, and Q. Lin, Isotopic characteristics of the post-orogenic granites from the northern China, and implication for crust growth, *Chin. Sci. Bull.*, *42*, 2188–2192, 1997.

Wu, H. R., Z. P. Pan, and C. Zhang, The Paleozoic stratigraphical sequence related to ophiolite and its discrimination of tectonic setting in western Junggar,in *New Improvement of Solid Geosciences in Northern Xinjiang* (in Chinese), edited by G. Z. Tu, pp. 151–162, Sci. Press, Beijing, 1993.

Xiao, X. C., Y. Q. Tang, J. Y. Li, M. Zhao, Y. M. Feng, and B. Q. Zhu, On tectonic evolution of the southern margin of the paleozoic composite megasuture zone, in *On Tectonic Evolution of the Southern Margin of the Paleozoic Composite Megasuture Zone* (in Chinese with English abstract), edited by X. C. Xiao and Y. Q. Tang, pp. 1–29, Beijing Technol. Press, Beijing, 1991.

Xu, J. F., H. J. Mei, X. Y. Yu, Z. H. Bai, H. C. Liu, F. R. Chen, Z. P. Zheng, and Q. Wang, Late Paleozoic subduction-related adakites in the northern margin of Junggar: Partial melting products of subducting slab, *Chin. Sci. Bull.*, *46*, 684–688, 2001.

Yin, A., and S. Y. Nie, A Phanerozoic palinspastic reconstruction of China and its neighboring regions, in *The Tectonic Evolution of Asia*, edited by A. Yin and T. M. Harrison, pp. 442–485, Cambridge Univ. Press, New York, 1996.

Zhang, C., M. Zhai, M. B. Allen, A. D. Saunders, G. Wang, and X. Huang, Implications of Paleozoic ophiolites from Western Junggar, NW China, for the tectonics of central Asia, *J. Geol. Soc. London*, *150*, 551–561, 1993.

Zhang, C., X. Huang, and M. G. Zhai, Geological characteristics of the ophiolites, and their tectonic settings and ages, western Junggar, Xinjiang (in Chinese), *Bull. Inst. Geol. Chin. Acad. Sci., Sci. Press*, 165–218, 1995.

Zhang, L. F., $^{40}Ar/^{39}Ar$ age and its geological significance of the blueschists from the western Junggar, Xinjiang, *Chin. Sci. Bull.*, *42*, 2178–2181, 1997.

Zhang, Q., and G. Q. Zhou, *Ophiolites of China* (in Chinese with English abstract), 182 pp., Sci. Press, Beijing, 2001.

Zhu, B. Q., L. S. Wang, and L. X. Wang, The Paleozoic ophiolites in the southwestern Junggar region (in Chinese with English abstract), *Bull. Xi'an Inst. Geol. Mineral Resour. Chin. Acda. Geol. Sci.*, *17*, 3–64, 1987.

J. Hao, Q. Hou, J. Li, K. Qin, S. Sun, Z. Wang, and W. Xiao, Laboratory of Lithosphere Tectonic Evolution, Institute of Geology and Geophysics, Chinese Academy of Sciences, Beijing, People's Republic of China. (z-hwang@mail.igcas.ac.cn)